An enhanced energy efficiency scheme for secure computing in UAV-MEC networks

Jin Qian, Xinmei Gao, Qinghe Gao, Hui Li, Yan Huo, Xiaoshuang Xing

An enhanced energy efficiency scheme for secure computing in UAV-MEC networks

Jin Qian

School of Information Engineering,
Taizhou University,
Taizhou, 225300, China
Email: qianjin@tzu.edu.cn

Xinmei Gao and Qinghe Gao*

School of Electronic and Information Engineering,
Beijing Jiaotong University,
Beijing, 100044, China
Email: 20120042@bjtu.edu.cn
Email: qhgao@bjtu.edu.cn
*Corresponding author

Hui Li

School of Information Engineering,
Taizhou University,
Taizhou, 225300, China
Email: huili_tzxy@tzu.edu.cn

Yan Huo

School of Electronic and Information Engineering,
Beijing Jiaotong University,
Beijing, 100044, China
Email: yhuo@bjtu.edu.cn

Xiaoshuang Xing

School of Computer Science and Engineering,
Changshu Institute of Technology,
Suzhou, 215506, China
Email: xing@cslg.edu.cn

Abstract: Mobile edge computing (MEC) mitigates terminal device computing demands by deploying cloud resources at the network's edge. In this MEC framework, unmanned aerial vehicles (UAVs) equipped with MEC servers enhance both uplink and downlink offloading due to their exceptional maneuverability and line-of-sight (LoS) connectivity. However, the wireless nature of UAV-MEC systems exposes sensitive data to potential eavesdropping. To address this concern, we formulate an optimisation challenge aimed at maximising data secrecy energy efficiency. This optimisation balances data and energy efficiency while preserving communication security. Due to the problem's time-varying and non-convex nature, we decompose it into four subproblems: terminal scheduling, local computing ratio, UAV transmit power, and UAV trajectory optimisation. Subsequently, we develop a hybrid iterative algorithm to maximise data secrecy energy efficiency during offloading. Simulations illustrate the algorithm can efficiently utilise terminal and MEC server computation capabilities, enhance system security, and improve energy efficiency while reducing energy consumption in task offloading.

Keywords: UAV-enabled mobile edge computing; physical layer security; PLS; UAV trajectory optimisation; energy efficiency.

Biographical notes: Jin Qian received his PhD in Communication and Information System from the Beijing Jiaotong University, Beijing, China in 2017. He is currently a Lecturer of the School of Information Engineering, Taizhou University. His major research interests include wireless communication theory, vehicular ad hoc networks and physical layer security, network security.

Xinmei Gao is a graduate student majoring in Information and Communication Engineering at the School of Electronic and Information Engineering, Beijing Jiaotong University. Her research interests include wireless communication, physical layer security, and mobile edging computing.

Qinghe Gao received her PhD in Communication and Information System from the Beijing Jiaotong University, Beijing, China, in 2020. She was a Visiting Scholar with the Department of Computer Science, George Washington University, Washington, DC, USA, from 2015 to 2017. She is currently a faculty member with the School of Electronics and Information Engineering, Beijing Jiaotong University. Her research interests include physical layer security, energy efficient resource allocation schemes, energy harvesting, internet of things (IoT), and industrial IoT.

Hui Li received her PhD in Computer Science and Technology from the Beijing Jiaotong University, Beijing, China in 2021. She is currently a Lecturer of the School of Information Engineering, Taizhou University. Her major research interests include security and privacy protection, vehicular ad hoc networks and edge computing.

Yan Huo received his PhD in Communication and Information System from the Beijing Jiaotong University, Beijing, China, in 2009. He was a Visiting Scholar with the Department of Computer Science, The George Washington University, from 2015 to 2016. He is currently a Professor with the School of Electronics and Information Engineering, Beijing Jiaotong University. His current research focuses on wireless communications, security and privacy, and signal processing.

Xiaoshuang Xing received her PhD in Communication and Information System from the Beijing Jiaotong University, Beijing, China in 2014. She is currently a Professor of the School of Information Engineering, Changshu Institute of Technology. Her major research interests include internet of things, vehicular network, physical layer security, cognitive radio networks, and spectrum prediction.

1 Introduction

The mobile edge computing (MEC) technology proposes the deployment of cloud resources with storage and processing capabilities at the edge of the radio access network (RAN) (Zhang et al., 2020). With its distributed, decentralised nature, low latency, and high computational capacity, MEC efficiently processes the massive data generated by IoT devices near the data sources, thus supporting mobile cloud computing (MCC). This approach reduces congestion in the core network, enhances resource efficiency, increases the security of sensitive data, and significantly streamlines the functionality of IoT devices, making them cost-effective. MEC technology has garnered significant attention from both the scientific community and industry due to its ability to greatly enhance the computational capacity of mobile devices in a cost-effective and energy-efficient manner. Applications span across domains like autonomous driving, virtual reality, smart grids, and intelligent factories (Spinelli and Mancuso, 2021). MEC brings computational resources closer to the edge of the network, allowing devices to offload computational tasks to edge servers for processing and receiving the results. Since MEC servers are typically deployed around devices, they can rapidly complete computation tasks, resulting in high-quality wireless coverage.

Yet, ground-based MEC servers (such as base stations near mobile users) are situated at specific locations, exhibiting lower flexibility and poorer channel quality for non-line-of-sight (NLoS) links, which in turn restrict communication rates (Chen et al., 2023; Corcoran and Datta, 2016). Moreover, in emergency scenarios such as earthquakes, traffic congestion, or crowded events, network infrastructure might be damaged due to natural disasters, or insufficient computing and communication resources in edge servers can lead to communication disruptions. Unmanned aerial vehicles (UAVs), characterised by their flexible deployment and resilience to natural disasters, hold the potential to be integral components of integrated sky-ground networks.

To address the issue of poor signal quality for NLoS links in ground-based MEC servers, there is a pressing need for the deployment of flexibly positioned MEC servers. UAVs, due to their agility, offer an ideal platform for executing edge computing tasks. UAVs equipped with various payloads, such as small-scale base stations and embedded computing modules, can adjust their positions based on the locations and densities of IoT devices, thereby maximising the execution of offloaded computational tasks.

UAVs can also establish line-of-sight (LoS) links by hovering above devices, significantly enhancing service quality. Consequently, deploying UAV-based MEC servers and designing UAV trajectories can significantly enhance the flexibility of MEC services. Furthermore, UAVs are easy to deploy and can swiftly provide temporary communication during natural disasters.

Intuitively, the openness of LoS links might lead to the leakage of sensitive and private information in UAV edge network data (Dang-Ngoc et al., 2022). Traditional approaches for ensuring wireless communication security are cryptography-based, which may result in high key management costs and computational complexities. In this paper, we introduce the idea of physical layer security (PLS) into a UAV-MEC network to serve as an effective supplement to higher-layer security mechanisms (Huo et al., 2018), leverage channel information to enhance transmission security, and maximise data secrecy energy efficiency (DSEE). DSEE The main contributions of this paper are summarised as follows.

- We formulate the UAV-MEC communication model based on RSCS-OFDM-DM technology, define a new metric, DSEE, to simultaneously characterise the secrecy and energy consumption of the UAV-MEC system, and present the maximisation problem of DSEE in the UAV-assisted MEC system.

- We decompose the DSEE maximisation problem into four subproblems, including terminal device (TD) scheduling, local computation ratio, UAV transmit power allocation, and UAV three-dimensional trajectory design. Also, we propose a hybrid iterative algorithm leveraging the sequential convex approximation (SCA) and alternating optimisation (AO) methods to find the optimal solution for the optimisation problem.

- We provide numerous simulation results to compare the security performance of the proposed approach with other benchmark schemes, including the optimal UAV trajectory, local computing ratio, convergence, and the maximum transmit power of UAV.

The rest of the paper is organised as follows. Related work is described in Section 2. Our UAV-MEC network model shown in Figure 1, the corresponding energy and latency model, and problem formulation are detailed in Section 3. Next, we analyse the proposed DSEE problem from four perspectives, i.e., terminal scheduling, local computation ratio, transmit power, and UAV trajectories in Section 4. Also, we present a hybrid iterative algorithm to find the optimal solution of the proposed problem in this section. Discussion of numerical results and conclusion with future research are provided in Sections 5 and 6, respectively.

2 Related work

The characteristics of high mobility, flexible deployment, and resilience to natural disasters make UAV communication systems increasingly important in 5G and beyond networks. UAVs and mobile communication technologies are mutually beneficial. On one hand, UAVs, as agile platforms, assist cellular networks in achieving massive connectivity and ubiquitous coverage requirements. On the other hand, UAVs also need to connect to cellular networks; advancements in ground-based cellular networks can provide UAVs with higher data rates, facilitating the development of applications such as real-time video surveillance. While UAV communication offers significant advantages, it is also susceptible to malicious attacks. On one hand, UAVs' elevated flight altitudes often lead to strong LoS connections between ground nodes or other aerial nodes. Primary air-to-ground (A2G) or air-to-air (A2A) links are favourable for legitimate communication but also provide opportunities for attackers. Attackers can exploit LoS propagation to enhance eavesdropping quality or increase interference efficiency. On the other hand, UAVs might share frequency bands with other systems in certain situations. A multitude of users from different systems operating on the same frequency band can lead to interference and privacy concerns. Consequently, communication security techniques within UAV systems are gaining increasing attention from both academia and industry. Unlike ground-based communication infrastructure, UAVs typically have stricter constraints on their onboard power and computational capabilities. Furthermore, due to the high mobility of UAV communication networks, their topology can be highly dynamic. Considering these factors, applying upper-layer encryption-based solutions for secure UAV communication may have practical limitations.

PLS is considered a promising approach for achieving information security with low computational complexity. In recent years, the application of PLS technology in UAV communication has attracted increasing research interest (Huo et al., 2019; Alanazi, 2021,?). In the context of UAV PLS communication, several important new issues need to be specifically considered (Wu et al., 2018b; Wen et al., 2023). First, the mobility of UAVs introduces a new dimension for optimisation, which is the position or trajectory of the UAV. Indeed, position optimisation and trajectory planning are integral components of research related to UAV PLS. Second, A2G/A2A channels exhibit different characteristics compared to ground-based channels. The distribution of aerial nodes might take new forms, such as within a three-dimensional (3D) sphere constrained by minimum node spacing. Analysing and designing in such scenarios may require consideration of new physical conditions. For example, the random jitter of UAVs can affect channel characteristics, posing challenges to acquiring accurate channel state information (CSI) (Wu et al., 2020, 2021). Third, UAV systems generally have limited energy resources, making energy efficiency even more crucial. In energy-constrained systems like the internet of things, energy efficiency is a common design goal that has been widely studied. However, the energy consumption of UAVs is closely related to their speed and acceleration, resulting in stricter overall energy constraints. Additionally,

factors such as the UAV's actual mobility and trajectory design need to be taken into account. Therefore, new power consumption models must consider these practical issues. Finally, the presence of actual dynamic models and no-fly zones introduces new constraint conditions for feasible UAV trajectory optimisation (Xu et al., 2020).

According to the roles that UAVs may play, PLS scenarios can be divided into the following categories: UAVs acting as communication nodes (transmitters or receivers), UAVs acting as collaborators (friendly jammers or relays), UAVs acting as attackers (malicious jammers or eavesdroppers), and UAVs acting as hiders or monitors (concepts of covert communication).

1   UAVs act as communication nodes: UAVs can serve as legitimate transmitters or receivers. Wang and Zhang (2020) employed AO and SCA techniques to jointly optimise user scheduling, UAV transmit power, and UAV trajectory, enhancing the UAV's secrecy rate. Zhang et al. (2019) considered joint optimisation of UAV trajectory and transmit power for both uplink and downlink scenarios to maximise the average secrecy rate (ASR). Xu et al. (2018) investigated energy efficiency in UAV-to-ground communication.

2   UAVs act as collaborators: In UAV communication systems, UAVs serving as friendly jammers or relays are regarded as collaborators within the UAV communication system. To enhance system security performance, UAVs can be utilised as friendly jammers, emitting jamming signals to confuse eavesdroppers (Li et al., 2019; Zhou et al., 2019a). In larger coverage UAV communication systems, due to energy constraints and the impact of path loss, introducing another UAV as a relay to amplify and forward signals becomes feasible (Shen et al., 2018; Shengnan et al., 2021; Lan et al., 2021). Li et al. (2019) considered a three-terminal ground eavesdropping system, where an interfering UAV collaboratively transmitted jamming signals to eavesdroppers. Some research work employed two UAVs as a base station and a friendly jammer respectively, deploying in cooperation with multiple users and eavesdroppers (Zhou et al., 2019a). Through joint optimisation of transmit power and trajectory for the two different roles of UAVs, the aim was to maximise the average security rate of all ground users, ensuring fairness among TDs. The research by the Shen and Shengnan teams focused on a scenario where a single UAV served as a relay in a UAV mobile relay system. In the presence of primary users and eavesdroppers, the UAV acted as a decoding and forwarding mobile relay to assist secure transmission from source nodes to legitimate destination nodes. This was achieved through block coordinate descent and convex programming methods, optimising UAV relay flight trajectory and transmit power to maximise security rates (Shen et al., 2018; Shengnan et al., 2021). The Lan team explored scenarios with multiple relays and eavesdroppers. To achieve secure cooperative amplification and forwarding of information from source to destination, simultaneous optimisation of relay trajectory, source, and relay transmit power was necessary to satisfy quality of service, thus maximising the average security rate (Lan et al., 2021).

3   UAVs act as attackers: Due to UAV's open A2G channels and flexible deployment, they become potent attackers. Abughalwa and Hasna (2019) compared eavesdropping performance in ground-based and aerial scenarios. Ye et al. (2018) studied the impact of UAV altitude on security performance. Wu et al. investigated high-risk areas for eavesdropping when UAVs perform directed transmissions over communication areas on the ground. These high-risk areas can be described as conical regions beneath the transmitter. To ensure PLS in scenarios where UAVs act as eavesdroppers, three-dimensional constraints on Eve's position need to be considered. Specifically, the design should avoid any occurrence of Eve within the conical region beneath the legitimate transmitter (Wu et al., 2018a). Furthermore, considering intelligent UAV attackers whose energy, position, or trajectory can be dynamically adjusted to maximise their attack efficiency, game-theoretic methods are often applied to analyse and design secure transmission in such cases (Li et al., 2020).

4   UAVs act as hiders or monitors: Covert communication, aiming to hide legitimate transmissions, and monitoring, aiming to identify unauthorised or malicious senders, are essential aspects of PLS research. The use of UAVs brings opportunities and challenges: the high probability of LoS links favours legitimate monitoring, making transmitter hiding more challenging (Zhou et al., 2019b; Jiang et al., 2021).

In this paper, we study the DSEE of the UAV-MEC system for the energy limitation during the offloading process caused by the limited battery capacity of ground terminal equipment. The main goal is to maximise the data tasks that can be processed per unit of energy while ensuring secure communication, thereby improving the energy efficiency of secure computation.

3   System model and problem formulation

3.1   A UAV-MEC network model

We consider a UAV-MEC secure communication system as shown in Figure 1. The system consists of a UAV-source S, K TDs with a single antenna, and E eavesdroppers with a single antenna. We assume that positions of TDs and eavesdroppers are known and static, defined as $\boldsymbol{u}_k = (x_k, y_k, 0)^T$ and $\boldsymbol{v}_e = (x_e, y_e, 0)^T$, respectively. Note that we consider that the UAV will travel from the takeoff point

L_I along a designated trajectory to land at the destination point L_F. The flight duration T can be discretised into N time slots, each of which is defined as δ_t, i.e., $T = N\delta_t$. Assuming δ_t is sufficiently small, each slot can be considered as uniform motion. Therefore, at $n \in \mathcal{N} \triangleq \{1, 2, ..., N\}$, the UAV's coordinates can be denoted as $L(n) \triangleq (x(n), y(n), h(n))^T$, and the distances between the UAV and TDs or eavesdroppers are defined as $r_k(n) = \|L(n) - u_k\|$ and $r_e(n) = \|L(n) - v_e\|$.

Figure 1 A UAV-MEC network model (see online version for colours)
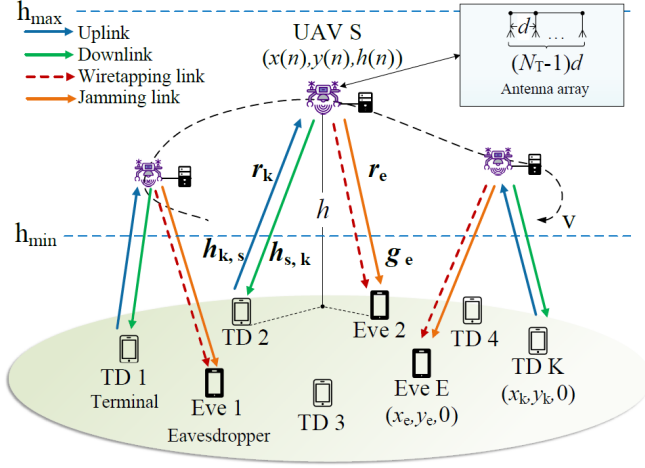
The UAV-MEC platform equipped with a N_T-element linear antenna array serves not only as the source for downlink signals but also employs the the random subcarrier selection-orthogonal frequency division multiplexing-direction modulation (RSCS-OFDM-DM) technique (Gao et al., 2022) to simultaneously transmit interference signals. This technique eliminates interference signals received by terminal devices, while eavesdroppers experience additional interference, thereby degrading their channel conditions. Let σ_2 denote the additive white Gaussian noise (AWGN) power. The signal-to-noise ratios (SNRs) for the uplink and downlink channels between the UAV and TDs, as well as the downlink eavesdropping channel, are expressed as follows.

$$\gamma_k^{up}(n) = \frac{h_k(n)p_{TU,k}(n)}{\sigma^2}, \tag{1}$$

$$\gamma_k^{down}(n) = \frac{h_k(n)p_{TUAV}(n)}{\sigma^2}, \tag{2}$$

$$\gamma_e(n) = \frac{g_e(n)p_{TUAV}(n)}{g_e(n)p_{JUAV}(n)\|H_e^H(n)w(n)\|^2 + \sigma^2}, \tag{3}$$

where $p_{TU,k}(n)$, $p_{TUAV}(n)$, and $p_{JUAV}(n)$ represent the transmit powers of TDs, UAV confidential signals, and UAV jamming signals in time slot n, respectively.

3.2 Energy and latency model

In the UAV-MEC system, we assume that the computational task of TD k in each time slot is denoted as A_k.

The limited computational capability of each terminal is represented as F_k^l. Let X_k^l be the number of CPU cycles required to process a bit-level computational task. The computational power of TD k, denoted as $p_{CU,k}$, is defined as the power consumption during computation, given by $p_{CU,k} = \kappa_0^l (F_k^l)^2$, where κ_0^l represents the effective switch capacitance of the CPU and its value depends on the chip architecture (Zhou et al., 2018; Cheng et al., 2018). Therefore, the local computational energy consumption of TD k in time slot n can be expressed as follows.

$$E_{CU,k}(n) = \alpha_k(n)A_k X_k^l p_{CU,k}$$
$$= \kappa_0^l \alpha_k(n)A_k X_k^l (F_k^l)^2. \tag{4}$$

And the computational latency is given by:

$$\tau_{CU,k}(n) = \frac{\alpha_k(n)A_k X_k^l}{F_k^l}. \tag{5}$$

When the computational task offloaded to the UAV is $(1 - \alpha_k(n))A_k$, the energy consumed during the offloading process can be calculated as follows.

$$E_{TU,k}(n) = m_k(n)\frac{(1 - \alpha_k(n))A_k}{R_k^{up}(n)} \times p_{TU,k}(n), \tag{6}$$

where $p_{TU,k}(n)$ is the transmit power of TD k which represents the fraction of the task that remains locally computed on TD k. It does not exceed the maximum transmit power of the device, $p_{TU,\max}$. And the corresponding transmission latency is given by

$$\tau_{TU,k}(n) = m_k(n)\frac{(1 - \alpha_k(n))A_k}{R_k^{up}(n)}. \tag{7}$$

Similarly, let X^{UAV} be the number of CPU cycles required to process a bit-level computational task in the UAV. The computational capability of the UAV is denoted as F^{UAV}, and its power consumption during computation is modeled as $p_{CUAV} = \kappa_0^{UAV}(F^{UAV})^2$, where κ_0^{UAV} represents the effective switch capacitance of the CPU, which depends on the chip architecture. Therefore, the energy consumption of the UAV during computation can be expressed as follows.

$$E_{CUAV}(n)$$
$$= m_k(n)(1 - \alpha_k(n))A_k X^{UAV} p_{CUAV}$$
$$= m_k(n)\kappa_0^{UAV}(1 - \alpha_k(n))A_k X^{UAV}(F^{UAV})^2. \tag{8}$$

And the computational latency on the UAV is given by:

$$\tau_{CUAV}(n) = m_k(n)\frac{(1 - \alpha_k(n))A_k X^{UAV}}{F^{UAV}}. \tag{9}$$

Assuming that the processed data size is A' and the result is returned to the TD. The downlink signal from the UAV includes both confidential signals and non-confidential ones. The power allocated for transmitting these two signals is denoted as $p_{TUAV}(n)$ and $p_{JUAV}(n)$, respectively. The power constraint is $p_{TUAV}(n) + p_{JUAV}(n) \leq P_s$, where P_s is the maximum transmit power of the UAV in each

time slot. Therefore, the energy consumed by the UAV for transmitting the confidential and interference signals is given by

$$E_{TUAV}(n) = m_k(n) \frac{A'}{R_k^{down}(n)} p_{TUAV}(n), \qquad (10)$$

$$E_{JUAV}(n) = m_k(n) \frac{A'}{\max R_{k,e}(n)} p_{JUAV}(n). \qquad (11)$$

3.3 Problem formulation

Considering the UAV-MEC model, we formulate an optimisation problem. The objective of this problem is to maximise DSEE during the computation offloading process. We jointly optimise the TD scheduling $M \triangleq \{m_k(n) \in \mathbb{R} \mid \forall k, \forall n\}$, local computation ratio $\alpha \triangleq \{\alpha_k(n) \in \mathbb{R} \mid \forall k, \forall n\}$, UAV transmit power $P_{UAV} \triangleq \{p_{TUAV}(n) \in \mathbb{R}, p_{JUAV}(n) \in \mathbb{R} \mid \forall n\}$, and UAV flight trajectory $L \triangleq \{L(n) \in \mathbb{R}^{3 \times 1} \mid \forall n\}$ in the UAV-assisted MEC system. Therefore, the maximisation problem of DSEE in the UAV-assisted MEC system can be formulated as follows.

$$\max_{M, \alpha, L, P_{UAV}} DSEE = \frac{\sum_{n=1}^{N} \sum_{k=1}^{K} DS(n)}{\sum_{n=1}^{N} \sum_{k=1}^{K} E_{total,k}(n)} \qquad (12a)$$

$$\text{s.t.} \sum_{k=1}^{K} m_k(n) = 1, m_k(n) \in \{0, 1\}, \qquad (12b)$$

$$L(1) = L_I, L(N+1) = L_F, \qquad (12c)$$

$$\|L(n+1) - L(n)\| \leq v_{\max} \delta_t, \qquad (12d)$$

$$h_{\min} \leq h(n) \leq h_{\max}, \qquad (12e)$$

$$p_{TUAV}(n) + p_{JUAV}(n) \leq P_s, \qquad (12f)$$

$$p_{TUAV}(n) \geq 0, \quad p_{JUAV}(n) \geq 0, \qquad (12g)$$

$$\tau_{CU,k}(n) + \tau_{TU,k}(n) + \tau_{CUAV}(n) \leq \delta_t, \qquad (12h)$$

$$0 \leq \alpha_k(n) \leq 1, \qquad (12i)$$

where $E_{total,k}(n) = E_{CU,k}(n) + E_{TU,k}(n) + E_{CUAV}(n) + E_{TUAV}(n) + E_{JUAV}(n)$ represents the total energy consumption of the entire system during the offloading process, which includes the energy consumption of local computation, uplink transmission, drone computation, and drone power transmission. The secure computational capacity $DS(n) = m_k(n) A_k (1 - \alpha_k(n)) [R_k^{down}(n) - \max R_{k,e}(n)]^+$ represents the security of the computational tasks offloaded to drones. Here, $[\cdot]^+ = \max\{\cdot, 0\}$.

Constraint (12b) is the TD scheduling constraint, which states that in the same time slot, only one TD can communicate with the drone. Constraints (12c), (12d) and (12e) impose limitations on the drone's flight start point, end point, maximum flight speed, and flight altitude. Constraints (12f) and (12g) restrict the power transmission of the drone. Constraint (12h) represents the maximum tolerable latency for each time slot when the kth TD communicates with the drone. Constraint (12i) represents the computational mode constraint for each TD in the system. When $\alpha_k = 1$, it signifies the local computation mode, while $\alpha_k = 0$ indicates the complete offloading mode.

4 Problem analysis and scheme design

Problem (12) is a non-convex mixed-integer fractional optimisation problem, which is challenging due to the following reasons. Firstly, binary variables are involved in both the objective function and constraint (12b). Secondly, both the numerator and denominator of the objective function are non-convex, resulting in a non-convex fractional objective function. Thus, we decompose the original problem into four subproblems, including TD scheduling optimisation, local computation ratio optimisation, transmit power optimisation, and UAV trajectory optimisation. Next, we present an efficient iterative algorithm by AO of the above four subproblems.

Algorithm 1   A scheduling selection algorithm

1: **Input:** $m_k(n) = 1$, $m_e(n) = 1, \forall n$;
2: **for** $n = 1$ to N **do**
3:     Find $k^* = \arg\max h_k(n)$
4:     Find $e^* = \arg\max g_e(n)$
5:     Set $m_{k^*}(n) = 1$, $m_{e^*}(n) = 1$, all others are set to 0.
6: **end for**

4.1 Terminal scheduling optimisation

Given the local computation ratio α, UAV trajectory L, and UAV transmit power P_{UAV}, equation (12) can be rewritten as follows.

$$\max_{M} \frac{\sum_{n=1}^{N} \sum_{k=1}^{K} DS(n)}{\sum_{n=1}^{N} \sum_{k=1}^{K} E_{total,k}(n)}$$
$$\text{s.t. equations (12b) and (12h)} \qquad (13)$$

It is evident that subproblem (13) is a binary variable integer optimisation problem, for which there are generally no efficient algorithms to solve directly. The traditional approach is to relax the binary variables into continuous variables and solve for a continuous solution. Then, the binary solution is reconstructed based on the continuous solution (Wu et al., 2018c). However, it cannot guarantee that the reconstructed binary solution is the optimal solution to subproblem (13). Moreover, mapping the continuous solution to the optimal binary solution is a highly challenging task with high computational complexity. In this subsection, we propose the scheduling selection algorithm Algorithm 1. Firstly, an additional binary variable $m_e(n) \in \{0, 1\}$ is introduced to represent Eve's eavesdropping scheduling, satisfying $\sum_{e=1}^{E} m_e(n) = 1, e \in \mathcal{E}, n \in \mathcal{N}$. Initially, all time slots for $m_k(n)$ and $m_e(n)$ are set to 1. Following the idea of exhaustive search, each time slot is traversed to find the optimal TD k^* or eavesdropper e^* for communication/eavesdropping channel, and their respective schedules are set to 1, while the schedules for other ground nodes are set to 0.

4.2 Local computation ratio optimisation

Given the scheduling value M, UAV trajectory L, and UAV transmit power P_{UAV}, we find the optimal local

computation ratio α. Based on the previous subsection, we determine the values of TD scheduling M. In time slot n, when $k \in \mathcal{K}\backslash\{k^*\}$, $m_k(n) = 0$, indicating that all computation tasks are executed locally and the local computation ratio is fixed as $\alpha_k(n) = 1$, requiring no further optimisation. Additionally, except for the local computation energy consumption, all other uplink transmission energy consumption, UAV computation energy consumption, and UAV transmit power consumption are zero, resulting in $E_{total,k}(n) = E_{CU,k}(n)$. When the TD is k^*, $m_{k^*}(n) = 1$, indicating that it offloads its task to the UAV-MEC platform. In this case, we need to solve for the value of $\alpha_{k^*}(n)$. Moreover, all energy consumptions have non-zero values, resulting in $E_{total,k}(n) = E_{total,k^*}(n)$. Therefore, equation (12) can be reformulated as follows.

$$\max_{\boldsymbol{\alpha}} \frac{\sum\limits_{n=1}^{N} \{A_{k^*}(1 - \alpha_{k^*}(n)) \left[R_{k^*}^{down}(n) - R_{k^*,e^*}(n)\right]^+\}}{\sum\limits_{n=1}^{N} \left[E_{total,k^*}(n) + \sum\limits_{k \in \mathcal{K}\backslash\{k^*\}} \kappa_0^l A_k X_k^l (F_k^l)^2\right]}$$

$$\text{s.t. } \tau_{CU,k^*} + \tau_{TU,k^*}$$
$$+ \frac{(1 - \alpha_{k^*}(n)) A_{k^*} X^{UAV}}{F^{UAV}} \leq \delta_t,$$
$$0 \leq \alpha_{k^*}(n) \leq 1 \tag{14}$$

where

$$E_{total,k^*}(n) = \kappa_0^l \alpha_{k^*}(n) A_{k^*} X_{k^*}^l (F_{k^*}^l)^2$$
$$+ \frac{(1 - \alpha_{k^*}(n)) A_{k^*}}{R_{k^*}^{up}(n)} \times p_{TU,k^*}(n)$$
$$+ \kappa_0^{UAV}(1 - \alpha_{k^*}(n)) A_{k^*} X^{UAV} (F^{UAV})^2$$
$$+ \frac{A'}{R_{k^*}^{down}(n)} p_{TUAV}(n)$$
$$+ \frac{A'}{R_{k^*,e^*}(n)} p_{JUAV}(n) \tag{15}$$

And constants in the objective function of subproblem (14) are as follows:

$$\begin{cases} C_1 = A_{k^*} \left[R_{k^*}^{down}(n) - R_{k^*,e^*}(n)\right]^+ \\ C_2 = \kappa_0^l A_{k^*} X_{k^*}^l (F_{k^*}^l)^2 \\ C_3 = \frac{A_{k^*}}{R_{k^*}^{up}(n)} \times p_{TU,k^*}(n) \\ C_4 = \kappa_0^{UAV} A_{k^*} X^{UAV} (F^{UAV})^2 \\ C_5 = \frac{A'}{R_{k^*}^{down}(n)} p_{TUAV}(n) + \frac{A'}{R_{k^*,e^*}(n)} p_{JUAV}(n) \\ \quad + \sum\limits_{k \in \mathcal{K}\backslash\{k^*\}} \kappa_0^l A_k X_k^l (F_k^l)^2 \end{cases}$$

Due to the presence of the optimisation variable $\alpha_{k^*}(n)$ in both the numerator and denominator of the objective function in subproblem (14), it leads to the non-convexity of the objective function. To address this, we can reformulate it as follows.

$$\max_{\boldsymbol{\alpha}} \sum_{n=1}^{N} [(C_1 + C_2)(1 - \alpha_{k^*})$$

$$+ (C_3 + C_4) \alpha_{k^*} + C_5]$$
$$\text{s.t. } \tau_{CU,k^*} + \tau_{TU,k^*}$$
$$+ \frac{(1 - \alpha_{k^*}(n)) A_{k^*} X^{UAV}}{F^{UAV}} \leq \delta_t,$$
$$0 \leq \alpha_{k^*}(n) \leq 1 \tag{16}$$

Obviously, the objective function of equation (16) is linear in its first derivatives, which makes it a convex optimisation problem.

4.3 Optimisation of transmit power for UAV

Given M, α, and L, we can solve following subproblem to optimise the UAV's transmit power P_{UAV}.

$$\max_{\boldsymbol{P}_{UAV}} \frac{\sum\limits_{n=1}^{N} \{A_{k^*}(1 - \alpha_{k^*}(n)) \left[R_{k^*}^{down}(n) - R_{k^*,e^*}(n)\right]^+\}}{\sum\limits_{n=1}^{N} \left[E_{total,k^*}(n) + \sum\limits_{k \in \mathcal{K}\backslash\{k^*\}} \kappa_0^l A_k X_k^l (F_k^l)^2\right]}$$

$$\text{s.t. equations (12f) and (12g)} \tag{17}$$

In subproblem (17), the optimisation variables are in $R_{k^*}^{down}(n)$, $R_{k^*,e^*}(n)$, $E_{TUAV}(n)$ and $E_{JUAV}(n)$. Since the value of the returned data A' is much smaller than the size of the offloaded data A_{k^*}, the variables $E_{TUAV}(n)$ and $E_{JUAV}(n)$ in the denominator of the objective function are also very small. As a result, the UAV transmit power can be approximated using the results from the previous iteration $\widetilde{p}_{TUAV}(n)$ and $\widetilde{p}_{JUAV}(n)$ to simplify the computation. Therefore, we have the following approximation.

$$\widetilde{E}_{total,k^*}(n) = E_{CU,k^*}(n) + E_{TU,k^*}(n) + E_{CUAV}(n)$$
$$+ \frac{A'}{R_{k^*}^{down}(n)} \widetilde{p}_{TUAV}(n)$$
$$+ \frac{A'}{R_{k^*,e^*}(n)} \widetilde{p}_{JUAV}(n) \tag{18}$$

The subproblem (17) can be further rewritten as follows.

$$\max_{\boldsymbol{P}_{UAV},\tau,\boldsymbol{\mu}} \frac{\tau}{\sum\limits_{n=1}^{N} \left[\widetilde{E}_{total,k^*}(n) + \sum\limits_{k \in \mathcal{K}\backslash\{k^*\}} \kappa_0^l A_k X_k^l (F_k^l)^2\right]}$$

$$\text{s.t. } \sum_{n=1}^{N} \{A_{k^*}(1 - \alpha_{k^*}(n)) \left[R_{k^*}^{down}(n) - \mu(n)\right]\} \geq \tau,$$
$$R_{k^*,e^*}(n) \leq \mu(n),$$
$$\text{equations (12f) and (12g)} \tag{19}$$

where τ and $\boldsymbol{\mu} \triangleq \{\mu(n) \in \mathbb{R} \mid n \in \mathcal{N}\}$ are two relaxation variables. However, the second constraint of (19) is still non-convex. Based on the SCA method, assuming

$\widetilde{p}_{TUAV}(n)$ is the result from the previous iteration, we can further transform $R_{k^*,e^*}(n)$ using a first-order Taylor expansion, i.e.,

$$R_{k^*,e^*}(n) \leq B \log_2 \left(1 + \frac{C_6 \widetilde{p}_{TUAV}(n)}{C_7(P_s - \widetilde{p}_{TUAV}(n)) + 1}\right)$$
$$+ \frac{B}{\ln 2} \times \frac{C_6(C_7 P_s + 1)}{[C_7(P_s - \widetilde{p}_{TUAV}(n)) + 1]}$$
$$\times \frac{(p_{TUAV}(n) - \widetilde{p}_{TUAV}(n))}{[C_7(P_s - \widetilde{p}_{TUAV}(n)) + 1 + C_6 \widetilde{p}_{TUAV}(n)]}$$
$$\triangleq \widehat{R}_{k^*,e^*}(n) \tag{20}$$

where

$$C_6 = g_{e^*}(n)/\sigma^2,$$
$$C_7 = \left[g_{e^*}(n)\|\boldsymbol{H}_e^H(n)\boldsymbol{w}(n)\|^2\right]/\sigma^2.$$

Accordingly, the second constraint of (19) can be transformed as follows.

$$\widehat{R}_{k^*,e^*}(n) \leq \mu(n) \tag{21}$$

And subproblem (19) satisfies the requirements of convex optimisation. We propose the UAV transmit power optimisation algorithm based on the SCA method, as shown in Algorithm 2.

Algorithm 2   A UAV transmit power optimisation algorithm

1: **Input:** $DSEE_{old} = 10^{(-7)}$, $tolerent = 10^{-3}$;
2: **for** $L = 1$ to 20 **do**
3:    Compute the optimal UAV launch power trajectory $\boldsymbol{P}_{UAV}$ by fixing $\boldsymbol{M}$, $\boldsymbol{\alpha}$, and $\boldsymbol{L}$ DSEE
4:    Set $DSEE = \frac{\tau}{\sum_{n=1}^{N}[\widetilde{E}_{total,k^*}(n) + \sum_{k \in \mathcal{K}\backslash\{k^*\}} \kappa_0^l A_k X_k^l (F_k^l)^2]}$
5:    **if** $|\frac{DSEE - DSEE_{old}}{DSEE_{old}}| \leq tolerent \parallel L \geq 20$ **then**
6:       Break
7:    **else**
8:       $DSEE_{old} = DSEE$
9:    **end if**
10: **end for**

4.4 Optimisation of UAV trajectories

To optimise UAV's trajectory, we reformulated equation (12) as the subproblem (22) when the TD scheduling $\boldsymbol{M}$, local computation ratio $\boldsymbol{\alpha}$, and UAV transmit power $\boldsymbol{P}_{UAV}$ are given.

$$\max_{\boldsymbol{L}} \frac{\sum_{n=1}^{N} \{A_{k^*}(1 - \alpha_{k^*}(n)) \left[R_{k^*}^{down}(n) - R_{k^*,e^{(n)}}\right]\}}{\sum_{n=1}^{N} \left[\widetilde{E}_{total,k^*}(n) + \sum_{k \in \mathcal{K}\backslash\{k^*\}} \kappa_0^l A_k X_k^l (F_k^l)^2\right]}$$

s.t. equations (12c), (12d), (12e) and (12h)   (22)

Obviously, the subproblem (22) is non-convex for the following reasons. Firstly, the UAV trajectory $\boldsymbol{L}$ involved in equation (12h) leads to a non-convex constraint set. Secondly, the UAV trajectory affects both the numerator and denominator of the objective function, making it difficult to directly solve this subproblem. Conventional convex forms cannot be used with CVX, so it is necessary to transform this non-convex subproblem into a convex problem using SCA.

The specific steps for solving the subproblem of UAV trajectory using the SCA method are as follows. Firstly, introduce two relaxation variables $\zeta_K \triangleq \{\xi_{k^*}(n) \mid \forall n\}$ and $\zeta_E \triangleq \{\xi_{e^*}(n) \mid \forall n\}$, and the subproblem (22) can be rewritten as follows.

$$\max_{\boldsymbol{L},\zeta_K,\zeta_E} \frac{\sum_{n=1}^{N} \{A_{k^*}(1 - \alpha_{k^*}(n)) \left[R_{k^*}^{down}(n) - R_{k^*,e^*}(n)\right]\}}{\sum_{n=1}^{N} \left[\widetilde{E}_{total,k^*}(n) + \sum_{k \in \mathcal{K}\backslash\{k^*\}} \kappa_0^l A_k X_k^l (F_k^l)^2\right]}$$

s.t. equations (12c), (12d) and (12e),
$$\xi_{k^*}(n) \geq \| \boldsymbol{L}(n) - u_{k^*} \|^2,$$
$$\xi_{e^*}(n) \leq \| \boldsymbol{L}(n) - v_{e^*} \|^2,$$
$$\xi_{k^*}(n) \geq h_{\min}^2 \tag{23}$$

Although $R_{k^*}^{down}$ is convex, the third constraint of subproblem (23) is non-convex in terms of $\boldsymbol{L}(n)$. Therefore, the subproblem (23) is still a non-convex optimisation problem. By using a first-order Taylor expansion, $R_{k^*}^{down}(n)$ can be approximated as follows.

$$R_{k^*}^{down}(n)$$
$$\geq B \log_2 \left(1 + \frac{\left[\frac{\beta_0 \eta_L \widetilde{P}_{k^*}^L(n)}{\widetilde{\xi}_{k^*}(n)^{\frac{\alpha_L}{2}}} + \frac{\beta_0 \eta_N \widetilde{P}_{k^*}^N(n)}{\widetilde{\xi}_{k^*}(n)^{\frac{\alpha_N}{2}}}\right] p_{TUAV}(n)}{\sigma^2}\right)$$
$$- \frac{B \log_2 \exp\left\{\frac{\alpha_L}{2} \frac{\beta_0 \eta_L \widetilde{P}_{k^*}^L(n)}{\widetilde{\xi}_{k^*}(n)^{\frac{\alpha_L}{2}+1}} + \frac{\alpha_N}{2} \frac{\beta_0 \eta_N \widetilde{P}_{k^*}^N(n)}{\widetilde{\xi}_{k^*}(n)^{\frac{\alpha_N}{2}+1}}\right\}}{\frac{\sigma^2}{p_{TUAV}(n)} + \left[\frac{\beta_0 \eta_L \widetilde{P}_{k^*}^L(n)}{\widetilde{\xi}_{k^*}(n)^{\frac{\alpha_L}{2}}} + \frac{\beta_0 \eta_N \widetilde{P}_{k^*}^N(n)}{\widetilde{\xi}_{k^*}(n)^{\frac{\alpha_N}{2}}}\right]}$$
$$\times (\xi_{k^*}(n) - \widetilde{\xi}_{k^*}(n)) \triangleq \widehat{R}_{k^*}^{down}(n) \tag{24}$$

Moreover, $\widetilde{P}_{k^*}^L(n)$ and $\widetilde{P}_{k^*}^N(n)$ represent the probabilities of LoS and NLoS links from the previous iteration, respectively. Similarly, $\widetilde{\xi}_{k^*}(n)$ corresponds to the value from the previous iteration. Consequently, the third constraint of (23) can be reexpressed as follows.

$$\xi_{e^*}(n) \leq \| \widetilde{\boldsymbol{L}}(n) - v_{e^*} \|^2$$
$$+ 2(\widetilde{\boldsymbol{L}}(n) - v_{e^*})^T (\boldsymbol{L}(n) - \widetilde{\boldsymbol{L}}(n)) \tag{25}$$

Therefore, we can find the optimal UAV trajectory when solve the subproblem (23) using Algorithm 3.

Algorithm 3 UAV trajectory optimisation

1: **Input:** $DSEE_{old} = 10^{(-7)}$, $tolerent = 10^{-3}$;
2: **for** $L = 1$ to 20 **do**
3:   **if** $L = 1$ **then**
4:     $\xi_{k^*} = r_{k^*}^2$
5:   **else**
6:     $\xi_{k^*} = \widetilde{\xi}_{k^*}$
7:   **end if**
8:   Computing the optimal UAV trajectory L by given M, α, and P_{UAV} in subproblem (23)
9:   Set $DSEE = \dfrac{\sum\limits_{n=1}^{N}\{A_{k^*}(1-\alpha_{k^*}(n))[\widehat{R}_{k^*}^{down}(n)-\max R_{k^*,e}(n)]\}}{\sum\limits_{n=1}^{N}[\widetilde{E}_{total,k^*}(n)+\sum\limits_{k\in\mathcal{K}\setminus\{k^*\}}\kappa_0^l A_k X_k^l (F_k^l)^2]}$
10:   **if** $|\frac{DSEE-DSEE_{old}}{DSEE_{old}}| \leq tolerent \parallel L \geq 20$ **then**
11:     Break
12:   **else**
13:     $DSEE_{old} = DSEE$
14:   **end if**
15: **end for**

4.5 Hybrid iterative algorithm

In this subsection, we design a hybrid iterative algorithm to solve problem (12). An AO method is first employed to decompose the original problem into four subproblems based on different sets of variables. For non-convex subproblems, the successive convex approximation method is used for solving. The subproblems are solved sequentially, and the iteration is repeated until the optimal solution is obtained. In the ith iteration, optimised values of M^i, α^i, P_{UAV}^i, and L^i are obtained in sequence. When one variable is optimised, the other variables are based on the results from the previous $i-1$ iterations. The details of Algorithm 4 are summarised.

5 Simulation

5.1 Parameter settings

In this section, the performance of the proposed scheme is evaluated through numerical simulations. Unless otherwise specified, simulation parameters are provided in Table 1. The implementation of algorithms and simulation procedures were conducted using the MATLAB platform and the CVX toolbox in this section.

Algorithm 4 A hybrid iterative algorithm

1: **Input:** Initial local computation ratio $\alpha^{(0)}$, initial UAV transmit power $P_{UAV}^{(0)}$, and initial 3D trajectory $L^{(0)}$;
2: Set the iteration index $i = 1$, the maximum number of iterations $L = 20$, and the threshold $\omega = 10^{-3}$
3: **repeat**
4:   Solve for the optimal TD scheduling M^i using **Algorithm 1**
5:   Fix M^i, P_{UAV}^{i-1}, and L^{i-1} to solve subproblem (16) and obtain the optimal local computation ratio α^i
6:   Fix M^i, α^i, and L^{i-1} to solve subproblem (19) and obtain the optimal UAV transmit power P_{UAV}^i
7:   Solve for the optimal UAV trajectory L^i using **Algorithm 3**
8:   Obtain the current optimal objective function value $DSEE^i$
9:   Update iteration index $i = i + 1$
10: **until** $(DSEE - DSEE_{old})/DSEE_{old} \leq \omega$ or $i > L$
11: **Output:** The optimal value $DSEE^i$

Table 1 Simulation parameter setting

Physical meaning	Value
Number of antennas N_T	4
Carrier frequency f_c	3 GHz
Subchannel bandwidth Δf	50 kHz
Channel gain β_0	–42 dB
Time slot δ_t	0.5 s
UAV maximum speed v_{max}	20 m/s
UAV minimum flying height h_{min}	100 m
UAV maximum flying height h_{max}	200 m
Noise power σ^2	–110 dBm
Channel environment factors a, b	20, 0.2
Excess path loss coefficient (LoS) η_L	–2.14 dB
Excess path loss coefficient (NLoS) η_N	–3.14 dB
Path loss exponent (LoS) α_L	2
Path loss exponent (NLoS) α_N	3
UAV flight period T	40 s
Terminal device transmit power $p_{TU,k}$	0.05 W
UAV maximum average transmit power P_s	1 W
Channel bandwidth B	20 MHz
Terminal device computation task size A_k	[10; 10; 10] Mbit
UAV downlink offloading task size A'	1 kbit
CPU cycle count X_k^l and X^{UAV}	1,000
Computation capacity F_k^l and F^{UAV}	500, 1,000 MHz
Capacitive switch κ_0^l and κ_0^{UAV}	$10^{(-27)}$

5.2 Results analysis

Figure 2 illustrates the optimised trajectory projections on the horizontal plane for UAVs with varying flight periods denoted by T. The dashed brown line represents the flight trajectory of the UAV when $T = 35$ s. Due to the requirement for the UAV to traverse from the starting point to the destination within the stipulated period, the flight duration of 35 s is insufficient, resulting in a predominantly linear flight path for the UAV. The solid blue line corresponds to the horizontal trajectory of the UAV at $T = 40$ s. The extension of the flight period allows the UAV to re-plan its flight route, aiming to approach the terminal device as swiftly as possible while adhering to imposed constraints. Obviously, the UAV's sensitivity to the eavesdropper's position is reduced. This discrepancy is attributed to the optimisation of the UAV's transmit power P_{UAV}, which rationally allocates the UAV's confidential signals and artificial noise (AN) to mitigate the eavesdropper's signal-to-interference-plus-noise ratio. The trajectory represented by the pink dotted line corresponds to the UAV's flight at $T = 60$ s. During this interval, the UAV has ample flight time, allowing it to hover above the TD for

a duration. At this point, the elevation angle between the UAV and the TD approaches 90°. This configuration yields a near-complete LoS channel probability close to 1. Such optimal channel conditions enable the achievement of the best channel state and the highest secure rate, contributing to enhanced security-computation energy efficiency.

Figure 2   The UAV trajectory (see online version for colours)
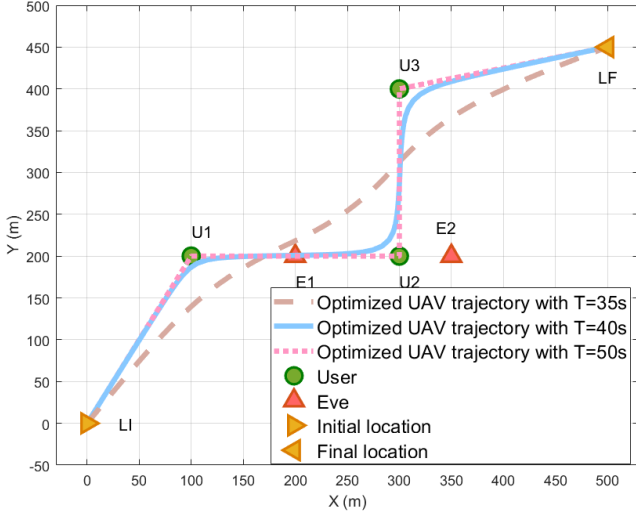
Figure 3   The UAV trajectory for various tasks
(see online version for colours)
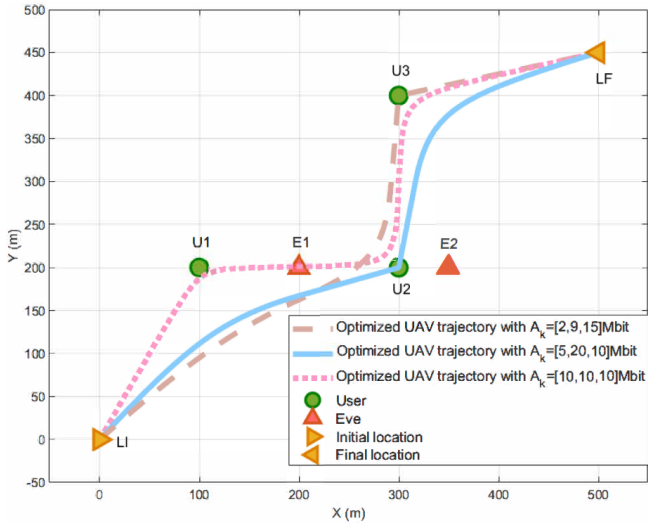
Figure 3 depicts UAV trajectories under different computational workloads of TDs. In Figure 4, the dashed brown lines represent UAV trajectories for TDs with computational workloads of $A_k = [2, 9, 15]$ Mbits, respectively. TD K_3 exhibits the highest computational workload of 15 Mbits, followed by K_2 and K_1. The UAV trajectory indicates a swift approach towards the vicinity of K_2, followed by a hovering period above K_3. Similarly, as depicted by the solid blue lines in Figure 3, when $A_k = [5, 20, 10]$ Mbits, the computational workload is higher for TD K_2, followed by K_3 and K_1. The UAV trajectory tends to approach K_2 and hover above it, while compared to K_1, the UAV trajectory approaches K_3 more closely. The

UAV's flight trajectory is influenced by the computational workload of the TDs. Higher computational workloads in the TDs enhance secure computation capabilities while also reducing the local computational energy consumption by offloading significant computational tasks. This ultimately improves DSEE. As a result, the UAV trajectory trend correlates positively with the computational workload of the TDs; UAV trajectories tend to approach TDs with higher computational workloads.

Figure 4   Scheduling of terminals and eavesdroppers
(see online version for colours)
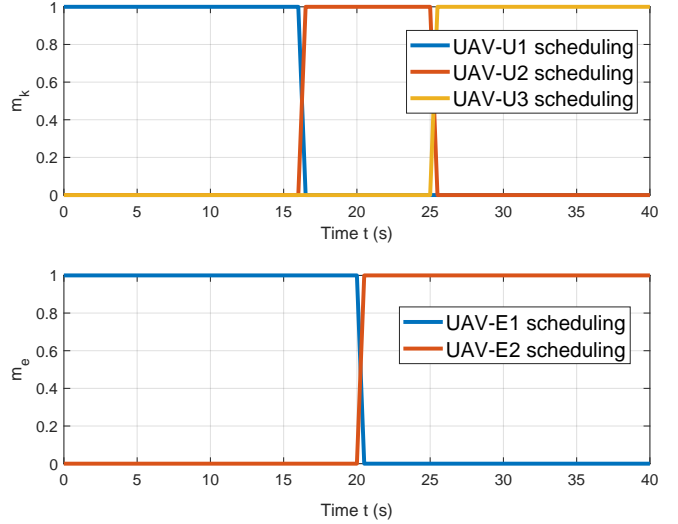
Figure 5   Local computing ratio (see online version for colours)
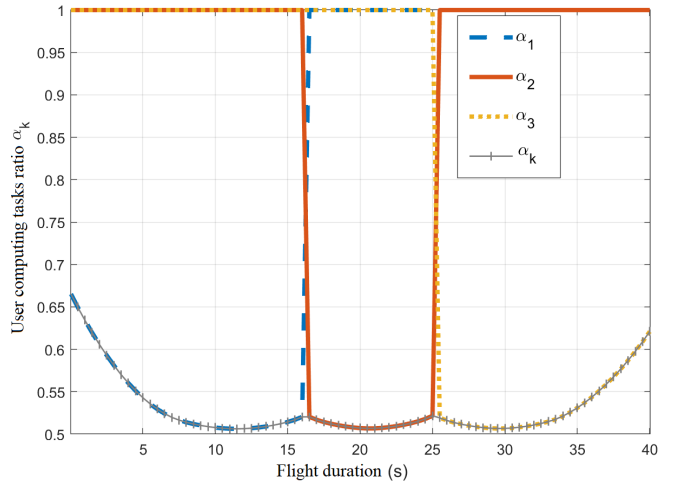
Figure 4 displays the scheduling of TDs and eavesdroppers at a flight period of $T = 40$ s. The TD scheduling diagram indicates that the UAV engages in communication with only one TD during a time slot, providing edge computing services. The eavesdropper scheduling diagram depicts the eavesdropper with the highest eavesdropping rate within each time slot. In general, whether it is TD scheduling or eavesdropper scheduling, the establishment of communication links is contingent on the distance between the UAV and the nodes. As the distance between the nodes and UAV decreases, the probability of establishing communication links increases.

Figure 6 TD transmit power (see online version for colours)
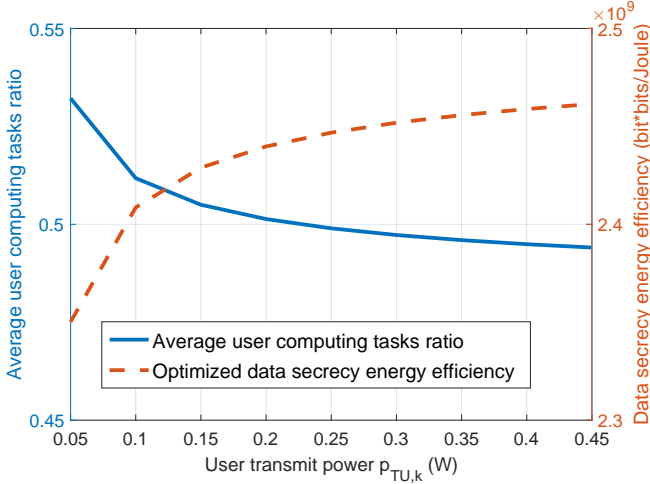
Figure 7 UAV transmit power when $T = 60$ s (see online version for colours)
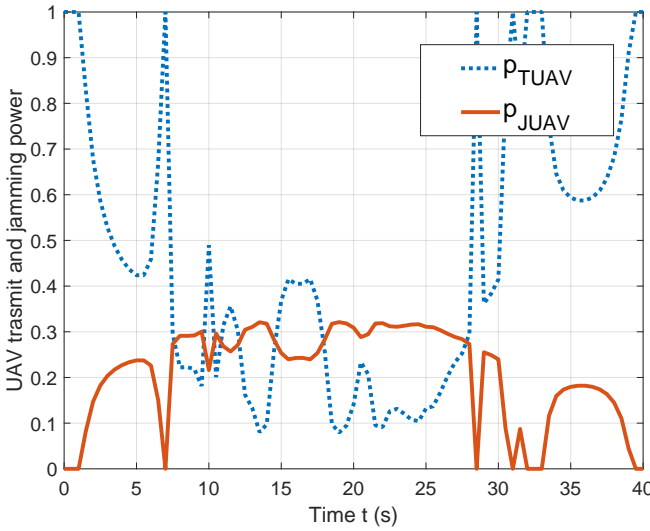
Figure 5 depicts the changes in the local computation ratio α_k for different TDs throughout a flight period, considering a transmit power of $P_{TU,k} = 0.05$ W for TD k. In comparison with Figure 5, the local computation ratio α_k is approximately inversely proportional to the TD scheduling $m_k(n)$. Taking the example of UAV-K_1 scheduling m_1 in Figure 4 and α_1 in Figure 5 from 0 to 17 seconds, m_1 remains 1, while α_1 forms a concave curve decreasing and then increasing. The lowest point of the curve occurs at 12 seconds, which represents the local computation ratio when the UAV is closest to K_1. After 17 seconds, when m_1 is entirely 0 and communication between the TD and UAV ceases, α_1 becomes all 1, indicating that computation tasks are executed locally on TD K_1. The same pattern applies to α_2 and α_3. In Figure 5, when TDs communicate with the UAV, the range of local computation ratio α_k remains between 0.5 and 0.7. More than half of the computation tasks are still executed locally. Meanwhile, Figure 6 illustrates the relationship between the average TD local computation ratio (average α_k when TDs communicate with the UAV)/DSEE and the TD transmit

power $P_{TU,k}$. The average TD local computation ratio decreases as $P_{TU,k}$ increases. With higher TD transmit power, devices are more inclined to offload computation tasks to the UAV, simultaneously increasing the amount of computation tasks offloaded and enhancing DSEE.

Figure 8 Convergence analysis (see online version for colours)
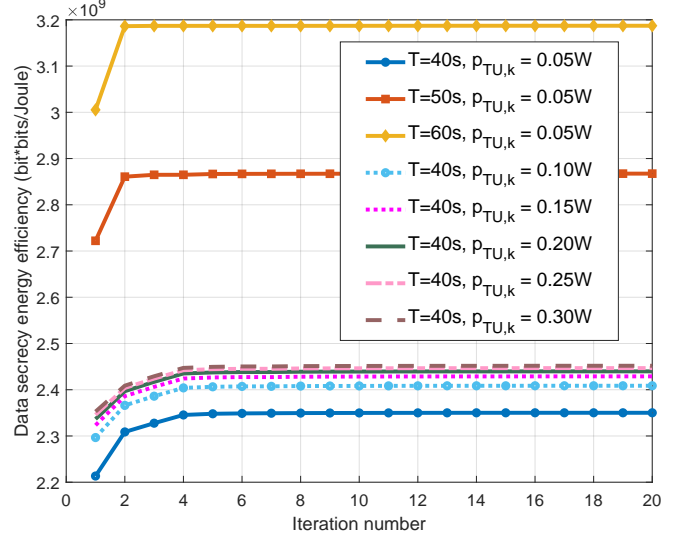
Figure 9 DSEE versus UAV maximum transmit power (see online version for colours)
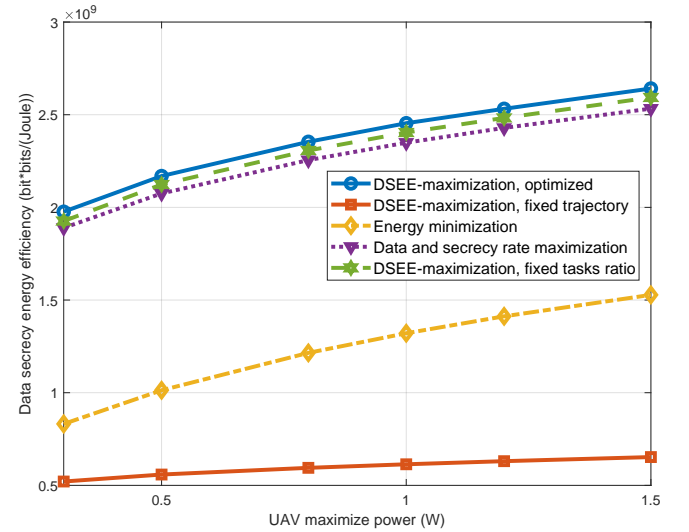
Figure 7 presents the allocation of transmit power for the UAV at a flight time of $T = 60$ s. The UAV's transmit power is composed of two components: the confidential signal transmit power p_{TUAV} and the AN transmit power p_{JUAV}. The overall trend of p_{TUAV} is a decrease followed by an increase, while p_{JUAV} initially increases and then decreases. Taking into account the analysis from Figure 2, during flight times of 12–19 s, 29.5–35 s and 45.5–49 s, the UAV hovers above K_1, K_2, and K_3, respectively. In these instances, the elevation angle between the ground terminal and the UAV is 90°, resulting in a LoS channel probability close to 1 and optimal communication channel conditions. Consequently, the UAV increases the transmit power of the confidential signal to enhance DSEE.

Figure 8 discusses the convergence of the proposed hybrid iterative algorithm under different flight times and varying TD transmit powers. The DSEE rapidly increases with an escalating number of iterations, eventually converging to a stable value after 2 to 4 iterations. The results indicate the algorithm's effective convergence to the optimal solution. When $p_{TU,k} = 0.05$ W and flight periods are $T = 40$ s, 50 s, and 60 s, a longer flight duration leads to quicker convergence and higher DSEE after convergence. This is due to the extended hovering time of the UAV over TDs as the flight period increases. Considering $T = 40$ s and comparing DSEE for different $p_{TU,k}$ values, as inferred from Figure 7, higher TD transmit power results in more computation tasks being offloaded to the UAV. Consequently, the post-convergence DSEE is higher. Evidently, the flight period has a much more significant impact on DSEE compared to TD transmit power.

Figure 9 validates the effectiveness of the hybrid iterative algorithm through a comparison of DSEE across various schemes. Firstly, the DSEE of this algorithm exhibits a monotonically increasing trend with the rise in the UAV's maximum transmit power P_s. It is evident that the influence of local computation ratio and secure computation capability on DSEE is relatively minor, while UAV trajectory and system energy have a more significant impact on DSEE. Furthermore, in comparison to other benchmark schemes, the proposed approach achieves a higher DSEE, highlighting its superiority.

6   Conclusions

In this paper, we define a new metric, DSEE, to characterise the secrecy and energy consumption of the UAV-MEC system. Using the metric, we intend to address the energy limitation challenge of ground terminals, while ensuring secure communication. We formulate an DSEE maximisation problem and analyse the problem from four perspectives, including terminal scheduling, UAV trajectory, UAV transmit power allocation, and local computing ratio. We designe a hybrid iterative algorithm based on SCA and AO to maximise the energy efficiency of system security calculations. Finally, we compare the secrecy performance of the proposed scheme with other benchmark to verify the superiority of the hybrid iterative algorithm proposed in this paper.

Acknowledgements

References

Abughalwa, M. and Hasna, M.O. (2019) 'A comparative secrecy study of flying and ground eavesdropping in UAV-based communication systems', in *2019 International Conference on Information and Communication Technology Convergence (ICTC)*, pp.416–421.

Alanazi, F. (2021) 'Physical layer security of cooperative wireless networks with RF energy harvesting', *International Journal of Sensor Networks*, Vol. 36, No. 3, pp.174–179.

Alanazi, F. (2021) 'Enhanced physical layer security using reconfigurable intelligent surfaces (RIS)', *International Journal of Sensor Networks*, Vol. 36, No. 4, pp.229–235.

Chen, J., Cao, X., Yang, P., Xiao, M., Ren, S., Zhao, Z. and Wu, D.O. (2023) 'Deep reinforcement learning based resource allocation in multi-UAV-aided MEC networks', *IEEE Transactions on Communications*, Vol. 71, No. 1, pp.296–309.

Cheng, K., Teng, Y., Sun, W., Liu, A. and Wang, X. (2018) 'Energy-efficient joint offloading and wireless resource allocation strategy in multi-MEC server systems', in *2018 IEEE International Conference on Communications (ICC)*, pp.1–6.

Corcoran, P. and Datta, S.K. (2016) 'Mobile-edge computing and the internet of things for consumers: extending cloud computing and services to the edge of the network', *IEEE Consumer Electronics Magazine*, Vol. 5, No. 4, pp.73–74.

Dang-Ngoc, H., Nguyen, D.N., Ho-Van, K., Hoang, D.T., Dutkiewicz, E., Pham, Q-V. and Hwang, W-J. (2022) 'Secure swarm UAV-assisted communications with cooperative friendly jamming', *IEEE Internet of Things Journal*, Vol. 9, No. 24, pp.25596–25611.

Gao, X., Huo, Y., Gao, Q., Zhao, H. and Ma, L. (2022) 'A secure downlink transmission scheme for a UAV-assisted edge network', *Wireless Communications and Mobile Computing*, April, pp.1–11.

Huo, Y., Fan, X., Ma, L., Cheng, X., Tian, Z. and Chen, D. (2019) 'Secure communications in tiered 5G wireless networks with cooperative jamming', *IEEE Transactions on Wireless Communications*, Vol. 18, No. 6, pp.3265–3280.

Huo, Y., Tian, Y., Ma, L., Cheng, X. and Jing, T. (2018) 'Jamming strategies for physical layer security', *IEEE Wireless Communications*, Vol. 25, No. 1, pp.148–153.

Jiang, X., Chen, X., Tang, J., Zhao, N., Zhang, X.Y., Niyato, D. and Wong, K-K. (2021) 'Covert communication in UAV-assisted air-ground networks', *IEEE Wireless Communications*, Vol. 28, No. 4, pp.190–197.

Lan, T., Hu, Z. and Zhang, Y. (2021) 'Improving physical layer security using multi-UAVs-enabled mobile relaying', in *2021 IEEE International Conference on Energy Internet (ICEI)*, pp.125–130.

Li, A., Wu, Q. and Zhang, R. (2019) 'UAV enabled cooperative jamming for improving secrecy of ground wiretap channel', *IEEE Wireless Communications Letters*, Vol. 8, No. 1, pp.181–184.

Li, C., Gao, Z., Xia, J., Deng, D. and Fan, L. (2020) 'Cache-enabled physical-layer secure game against smart UAV-assisted attacks in B5G NOMA networks', *EURASIP Journal on Wireless Communications and Networking*, Vol. 2020, No. 1, pp.1–9.

Shen, L., Wang, N. and Mu, X. (2018) 'Iterative UAV trajectory optimization for physical layer secure mobile relaying', in *2018 International Conference on Cyber-Enabled Distributed Computing and Knowledge Discovery (CyberC)*, pp.19–194.

Shengnan, C., Xiangdong, J., Yixuan, G. and Yuhua, Z. (2021) 'Physical layer security communication of cognitive UAV mobile relay network', in *2021 7th International Symposium on Mechatronics and Industrial Informatics (ISMII)*, pp.267–271.

Spinelli, F. and Mancuso, V. (2021) 'Toward enabled industrial verticals in 5G: a survey on MEC-based approaches to provisioning and flexibility', *IEEE Communications Surveys & Tutorials*, Vol. 23, No. 1, pp.596–630.

Wang, H-M. and Zhang, X. (2020) 'UAV secure downlink NOMA transmissions: a secure users oriented perspective', *IEEE Transactions on Communications*, Vol. 68, No. 9, pp.5732–5746.

Wen, Y., Liu, L., Li, J., Hou, X., Zhang, N., Dong, M., Atiquzzaman, M., Wang, K. and Huo, Y. (2023) 'A covert jamming scheme against an intelligent eavesdropper in cooperative cognitive radio networks', *IEEE Transactions on Vehicular Technology*, Vol. 72, No. 10, pp.1–12.

Wu, Y., Yang, W. and Sun, X. (2018a) 'Securing UAV-enabled millimeter wave communication via trajectory and power optimization', in *2018 IEEE 4th International Conference on Computer and Communications (ICCC)*, pp.970–975.

Wu, Y., Khisti, A., Xiao, C., Caire, G., Wong, K-K. and Gao, X. (2018b) 'A survey of physical layer security techniques for 5G wireless networks and challenges ahead', *IEEE Journal on Selected Areas in Communications*, Vol. 36, No. 4, pp.679–695.

Wu, Q., Zeng, Y. and Zhang, R. (2018c) 'Joint trajectory and communication design for multi-UAV enabled wireless networks', *IEEE Transactions on Wireless Communications*, Vol. 17, No. 3, pp.2109–2121.

Wu, H., Wen, Y., Zhang, J., Wei, Z., Zhang, N. and Tao, X. (2020) 'Energy-efficient and secure air-to-ground communication with jittering UAV', *IEEE Transactions on Vehicular Technology*, Vol. 69, No. 4, pp.3954–3967.

Wu, H., Li, H., Wei, Z., Zhang, N. and Tao, X. (2021) 'Secrecy performance analysis of air-to-ground communication with UAV jitter and multiple random walking eavesdroppers', *IEEE Transactions on Vehicular Technology*, Vol. 70, No. 1, pp.572–584.

Xu, D., Sun, Y., Ng, D.W.K. and Schober, R. (2020) 'Multiuser miso UAV communications in uncertain environments with no-fly zones: robust trajectory and resource allocation design', *IEEE Transactions on Communications*, Vol. 68, No. 5, pp.3153–3172.

Xu, J., Zeng, Y. and Zhang, R. (2018) 'UAV-enabled wireless power transfer: trajectory design and energy optimization', *IEEE Transactions on Wireless Communications*, Vol. 17, No. 8, pp.5092–5106.

Ye, J., Zhang, C., Pan, G., Chen, Y. and Ding, Z. (2018) 'Secrecy analysis for spatially random UAV systems', in *2018 IEEE Globecom Workshops (GC Wkshps)*, pp.1–6.

Zhang, G., Wu, Q., Cui, M. and Zhang, R. (2019) 'Securing UAV communications via joint trajectory and power control', *IEEE Transactions on Wireless Communications*, Vol. 18, No. 2, pp.1376–1389.

Zhang, Q., Gui, L., Hou, F., Chen, J., Zhu, S. and Tian, F. (2020) 'Dynamic task offloading and resource allocation for mobile-edge computing in dense cloud ran', *IEEE Internet of Things Journal*, Vol. 7, No. 4, pp.3282–3299.

Zhou, F., Wu, Y., Hu, R.Q. and Qian, Y. (2018) 'Computation rate maximization in UAV-enabled wireless-powered mobile-edge computing systems', *IEEE Journal on Selected Areas in Communications*, Vol. 36, No. 9, pp.1927–1941.

Zhou, X., Wu, Q., Yan, S., Shu, F. and Li, J. (2019a) 'UAV-enabled secure communications: joint trajectory and transmit power optimization', *IEEE Transactions on Vehicular Technology*, Vol. 68, No. 4, pp.4069–4073.

Zhou, X., Yan, S., Hu, J., Sun, J., Li, J. and Shu, F. (2019b) 'Joint optimization of a UAV's trajectory and transmit power for covert communications', *IEEE Transactions on Signal Processing*, Vol. 67, No. 16, pp.4276–4290.